Journal of Molecular Liquids 370 (2023) 120872

Contents lists available at ScienceDirect

Journal of Molecular Liquids

journal homepage: www.elsevier.com/locate/molliq

Sequestration of Np^{4+} and NpO_2^{2+} ions by using diglycolamide-functionalized azacrown ethers in $C_8mim{\cdot}NTf_2$ ionic liquid: Extraction, spectroscopic, electrochemical and DFT studies

Rajesh B. Gujar [a], Parveen K. Verma [a], Bholanath Mahanty [a], Arunasis Bhattacharyya [a], Sk. Musharaf Ali [b], Richard J.M. Egberink [c], Jurriaan Huskens [c], Willem Verboom [c,*], Prasanta K. Mohapatra [a,*]

[a] Radiochemistry Division, Bhabha Atomic Research Centre, Mumbai 400 085, India
[b] Chemical Engineering Division, Bhabha Atomic Research Centre, Mumbai 400085, India
[c] Laboratory of Molecular Nanofabrication, Department for Molecules & Materials, MESA+ Institute, University of Twente, P.O. Box 217, 7500 AE Enschede, the Netherlands

ARTICLE INFO

Article history:
Received 22 July 2022
Revised 23 October 2022
Accepted 22 November 2022
Available online 26 November 2022

Keywords:
Neptunium
Diglycolamide
Azacrown ethers
Ionic liquid
Solvent-extraction
Complexation

ABSTRACT

Complexation of Np^{4+} and NpO_2^{2+} ions was studied in a room temperature ionic liquid ($C_8mim{\bullet}NTf_2$) using two multiple diglycolamide (DGA) ligands with three and four DGA arms tethered to the nitrogen atoms of the aza-9-crown-3 and -12-crown-4 scaffolds termed as $\mathbf{L_I}$ and $\mathbf{L_{II}}$, respectively. The studies include solvent extraction, UV–visible spectrophotometry, cyclic voltammetry, and density functional theory (DFT). While the extraction of NpO_2^{2+} ion, as a function of the nitric acid concentration, resembled that of the 'solvation' mechanism, seen in case of neutral donor ligands in molecular diluent, an opposite trend was observed for the Np^{4+} ion suggesting a 'cation-exchange' mechanism often operating in the case of ionic liquid-based solvent systems. Slope analysis suggested formation of $Np(NO_3)]^{3+}{\bullet}L$ and $NpO_2(NO_3)_2{\bullet}L$ extracted species for the extraction of Np^{4+} and NpO_2^{2+}, respectively, in both the ligand systems. The complexation of the metal ions was supported by peak shifts in the UV–visible spectrophotometric as well as cyclic voltammetric studies. DFT studies were carried out to get structural information of the complexes.

© 2022 Elsevier B.V. All rights reserved.

1. Introduction

Out of the various transuranium elements, neptunium is formed in significant quantities in the nuclear reactors and, hence, is also present as a major component of the total minor actinides in the dissolver solution [1]. Neptunium primarily exists as Np(V) or NpO_2^+, which is the least extractable form of Np in the PUREX process and, as a consequence, a significant quantity of it passes to the PUREX raffinate and subsequently to the high level liquid waste (HLLW) [1]. The concentration of Np, in the HLLW of pressurized water reactor (PWR) origin (burn up: 33,000 MWd/T) is ca. 0.067 mg/g, which is mainly due to its longest lived isotope ^{237}Np ($t_{1/2}$: 2.1×10^6 y) [2,3]. The safe management of the nuclear waste is of prime importance for human welfare and public acceptability of the nuclear energy as an alternative source of the fossil fuel driven economy [1,4]. Considering, the long half-life of ^{237}Np and high mobility of NpO_2^+ (in the case of any leaching from deep geological repository or nuclear accidents) in the environmental media [5,6], significant efforts are needed to develop efficient novel separation methods for ^{237}Np removal from the HLLW [1]. Besides reducing the ^{237}Np associated long-term radiotoxicity, adopting the 'actinide partitioning' strategy for the selective removal of minor actinides along with ^{237}Np will also significantly reduce the surveillance period of the repositories [4,7,8]. The recovered ^{237}Np can also find application in the production of ^{238}Pu for use in pace makers as well as for space applications [1].

The separation of Np has been attempted by different research groups using a host of extractants. Out of various amides, malonamides, diglycolamides (DGA), and phosphorous-based neutral extractants, the DGA-based ligands are reported to be the most efficient for the trivalent actinides, yielding very high extraction of the actinide ions at relatively low ligand concentrations at moderate HNO_3 concentrations [4,7,9]. Active research is being pursued in our group on DGA-based ligands for the selective and effective recovery of minor actinides from HLLW [4,8,10–16]. Several multiple DGA ligands were evaluated for the extraction of tri-, tetra- and

* Corresponding authors.
E-mail addresses: w.verboom@utwente.nl (W. Verboom), mpatra@barc.gov.in (P. K. Mohapatra).

https://doi.org/10.1016/j.molliq.2022.120872
0167-7322/© 2022 Elsevier B.V. All rights reserved.

hexavalent actinide from nitric acid medium using either molecular solvents or room temperature ionic liquids (RTILs) [15,17–22]. RTILs are non-flammable neoteric tailor-made diluents with low volatility and are being extensively studied for *f*-block metal ion extraction from a variety of feed conditions [23–27]. The wide electrochemical windows of RTIL also help in the direct electro winning of the extracted metal ions [28,29].

The selection of the solvent plays a key role, not only deciding the distribution ratio of the given metal ions, but also in the associated extraction mechanism and the selectivity of different metal ions. The extraction behavior of actinide ions using DGA-based ligands dissolved in molecular solvents or RTILs shows a difference in their extraction mechanism with mostly enhancement in the distribution ratio in case of a RTIL [30–32]. The tripodal ligands viz. DGA-TREN and T-DGA (Fig. 1) showed a unique selectivity reversal during the solvent extraction of trivalent actinide (Am^{3+}) and lanthanide (Eu^{3+}) ions in RTIL [18]. The extraction mechanism, when molecular solvents are used as the diluents is restricted to a solvation mechanism, but in the case of RTILs other extraction mechanisms are also possible [22]. The extraction mechanism for trivalent lanthanide / actinide ions in molecular diluents is based on reverse micelle formation having 3 to 4 TODGA molecules [33]. Based on this, several multiple DGA-based ligands such as calix[4]arenes [34], tripodals [35], pillar[5]arenes, azacrown [36] and dendrimers [29,37] were developed and investigated for the extraction of tri-, tetra- and hexavalent *f*-cations. Although there are several reports for the extraction of tri- and hexavalent *f*-cations using DGA-based ligands, the extraction of Np^{4+} is not extensively evaluated from acidic feeds as encountered in the HLLW [34,38–40]. We have reported the promising extraction of Np^{4+} employing DGA–functionalized dendrimer ligands [37,41] and DGA-functionalized azacrown ethers [42] in molecular diluents.

In view of the promising results reported with the DGA-based dendrimer ligands in C_4mim•NTf_2 compared to molecular diluents, it was of great relevance to evaluate two ligands with azacrown ether scaffolds tethered with DGA arms termed as $\mathbf{L_I}$ and $\mathbf{L_{II}}$ (Fig. 1(b)) in RTIL.

The present studies involve the extraction of Np^{4+} and NpO_2^{2+} using $\mathbf{L_I}$ and $\mathbf{L_{II}}$ dissolved in C_8mim•NTf_2 from nitric acid feed solutions. Batch solvent extraction, UV–visible spectrophotometric and theoretical studies were conducted to get an idea about the nature of the extracted species. Finally, cyclic voltammetric studies were carried out to get information about the relative donating strength of the ligands and to evaluate the diffusion coefficient and the activation energy of diffusion of the extracted complexes in C_8mim•NTf_2. To the best of our knowledge, this is the first report on the extraction of Np^{4+} and NpO_2^{2+} using azacrown-based DGAs in RTIL. The results may help in a better understanding of the extraction in a RTIL and contribute to designing suitable solvent systems that can be applied in radioactive waste management.

2. Experimental

2.1. Materials

The synthesis and characterization of the azacrown ether-based ligands $\mathbf{L_I}$ and $\mathbf{L_{II}}$ (Fig. 1) used in present studies have been described before [42,43]. C_8mim•NTf_2 was purchased from Iolictec, Germany. C_8mim.NTf_2 was decolorized prior to use by contacting with activated charcoal as described before [44]. HNO_3 solutions with different molarity were prepared by dilution of Suprapur grade HNO_3 (Merck, Germany). A standard NaOH solution (standardized using primary standard potassium hydrogen phthalate) was used for the preparation of dilute nitric acid solutions.

2.2. Neptunium radiotracers

^{239}Np tracer ($\sim 10^{-12}$ M) was prepared by the irradiation of solid $UO_2(NO_3)_2$ in the Dhruva reactor at a thermal neutron flux of 5×10^{13} n/cm^2/s for 5 days. ^{239}Np was subsequently separated from the bulk of uranium and other fission/activation products using the reported TTA (2-thenoyl trifluoroacetone) extraction method [16,45]. The oxidation of Np to NpO_2^{2+} was carried out using 10 μL of 2×10^{-2} M $K_2Cr_2O_7$ solution [28,46]. The valency of Np to Np^{4+} was adjusted using ferrous sulphamate (10 μL) and hydroxylamine (10 μL). The stability of the Np^{4+} state was tested by an HTTA extraction method as reported before [16,28,42].

2.3. Solvent extraction of actinide ions

The solvent extraction of Np^{4+} and NpO_2^{2+} ions was carried out by equilibrating equal volumes (usually 1 mL) of the C_8mim•NTf_2 phase containing 5×10^{-4} M $\mathbf{L_I}$ and 1×10^{-4} M $\mathbf{L_{II}}$ and aqueous phases containing ^{239}Np radiotracer at a given acidity in leak tight Pyrex glass tubes (10 mL capacity). After achieving the equilibration, the tubes were centrifuged at 5000 rpm for 2 min for good phase separation. Subsequently, 100 μL aliquots were removed from both the phases for the radiometric assay using NaI(Tl) (well type) scintillation detector (Para Electronics) coupled with a multi-channel analyzer (ECIL, India). The distribution ratio (D_{Np}) of Np^{4+} or NpO_2^{2+} was estimated as the ratio of activity per unit time per unit volume in the ionic liquid phase to that in the aqueous phase at a given acidity. The distribution experiments were carried out in triplicate and the reported data were within ±5 % of their average values. A thermostated water bath was used for the temperature variation studies and all other studies were carried out at 25 ℃. The time of equilibration was estimated by kinetic studies at 3 M HNO_3. For the kinetics studies, the D_{Np} was estimated for both metal ions by $\mathbf{L_I}$ and $\mathbf{L_{II}}$ at different time intervals at a given ligand and nitric acid concentration.

2.4. Cyclic voltammetry

The cyclic voltammetry (CV) studies for all Np^{4+} extract samples in the RTIL were done using an AUTOLAB (Metrohm, Switzerland) electrochemical work station. The data acquisition and analysis were performed using GPES (version 4.9) software provided with the instrument. All samples were purged with high purity N_2 gas for 10–15 min before the CV measurements. A constant N_2 atmosphere was maintained during the CV scans for all the samples. The CV studies were conducted in a three-electrode system with a glassy carbon (GC) working electrode (WE) (disk electrode with 1.5 mm dia) and platinum (Pt) counter electrode (CE) as well as reference electrode (RE) (disk electrode with 2 mm dia). The present experimental setup was selected based on our previous CV studies of Np in C_4mim•NTf_2 [28]. The CV was also recorded at different scan rates (0.05 V s^{-1} to 0.5 V s^{-1}) at different temperatures (15–45 ℃).

2.5. Computational methodology

Methyl (instead of *n*-octyl) derivatives of the DGA-containing ligands $\mathbf{L_I}$ and $\mathbf{L_{II}}$ were considered for the computational studies to avoid difficulties in convergence due to the C—C single bond rotations of the long hydrocarbon chains. All the DFT based studies were performed using the TURBOMOLE 7.2 program package [47–49]. The geometries of $\mathbf{L_I}$, $\mathbf{L_{II}}$ and their Np^{4+} and NpO_2^{2+} complexes were optimized by using the Becke's exchange functional [50] in conjunction with the Perdew's correlation functional [51] (BP86) with generalized gradient approximation (GGA). Sixty

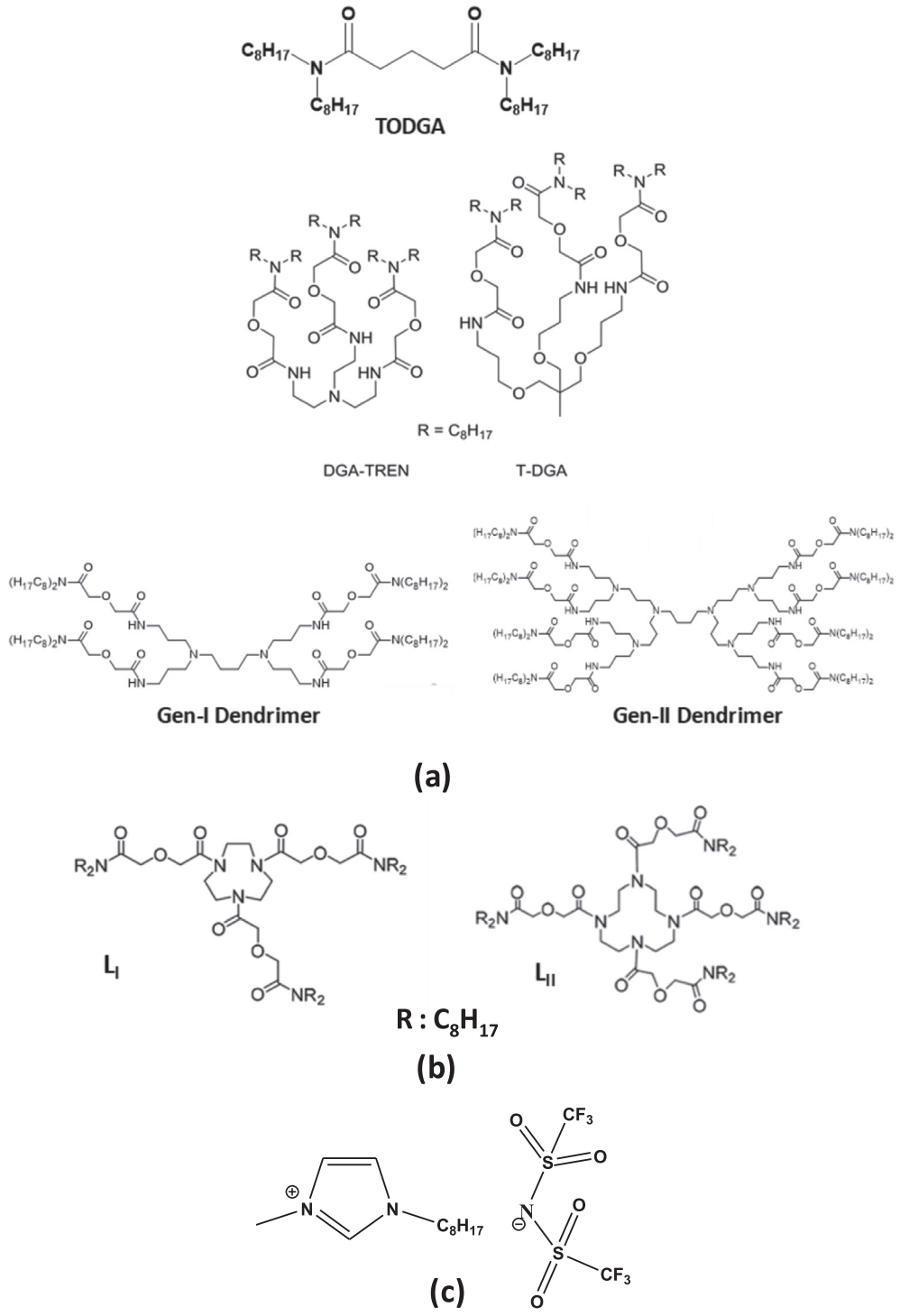

Fig. 1. (a) Structures of TODGA and other multiple DGA ligands; (b) DGA functionalized azacrown ether ligands $\mathbf{L_I}$ and $\mathbf{L_{II}}$ used in present studies and (c) $C_8mim{\bullet}NTf_2$.

electron core pseudo-potentials (ECPs) along with the corresponding def-SV(P) basis set, as implemented in the TURBOMOLE suit of program, were selected for the neptunium ion for the geometry optimization studies, whereas all the other lighter atoms were treated at the all electron (AE) level. Energies of the free ligand molecules and their complexes were calculated using hybrid B3LYP density functional [50,52] employing triple zeta valence plus polarization (TZVP) basis set [53,54] using equilibrated structures obtained at BP86/SVP level of theory as implemented in the TURBOMOLE suit of program.

3. Results and discussion

3.1. Extraction kinetics

The extraction kinetics of Np^{4+} and NpO_2^{2+} ions by $\mathbf{L_I}$ and $\mathbf{L_{II}}$ in the ionic liquid was found to be slower when compared to that in molecular diluents [42]. For both the ligands, the time required to attain equilibrium is ca. 3 h except for the Np^{4+}-$\mathbf{L_I}$ extraction system (Fig. 2). The relatively faster extraction kinetics for the Np^{4+}-$\mathbf{L_I}$ system may arise from the smaller cavity size of $\mathbf{L_I}$ compared to

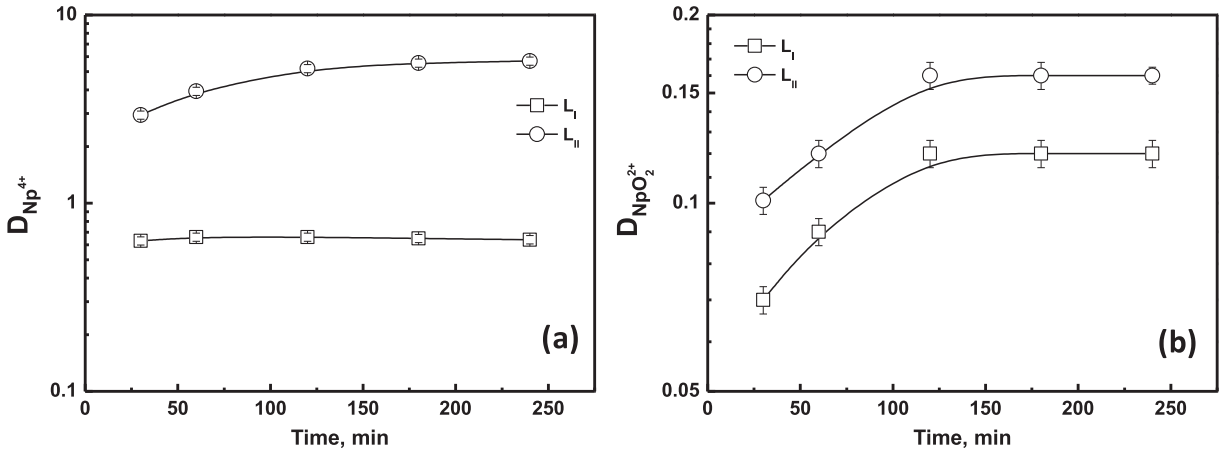

Fig. 2. Extraction kinetics of (a) Np^{4+} and (b) NpO_2^{2+} using [$\mathbf{L_I}$]: 5 × 10^{-4} M and [$\mathbf{L_{II}}$]: 1 × 10^{-4} M dissolved in C_8mim•NTf_2 at 3 M HNO_3; T: 298 K.

that of $\mathbf{L_{II}}$. On the other hand, the slower kinetics with $\mathbf{L_{II}}$ is attributed to the ligand conformation changes to accommodate both the ions irrespective of the overall shape and charge of them.

3.2. Effect of aqueous feed acidity of extraction of actinide ions

The extraction of Np^{4+} and NpO_2^{2+} with $\mathbf{L_I/L_{II}}$ dissolved in C_8mim•NTf_2 was studied as a function of the aqueous phase acidity. The extraction of these actinide ions by the RTIL alone (in the absence of any ligand) was reported to be very poor [55,56]. Hence, their extraction properties are governed by the ligand present in the RTIL phase. For the present system, extraction of Np^{4+} ions shows a 'cation-exchange' mechanism at lower acidity range, which changes to a 'solvation' or 'anion-exchange' mechanism at higher acidity (>2 M) for both the ligands (Fig. 3). A similar behavior for Np^{4+} ion extraction was reported for DGA-functionalized dendrimers in an ionic liquid [29]. The 'cation-exchange' mechanism for extraction of Np^{4+} was also observed by others for neutral extractants dissolved in an ionic liquid [40,57,58]. The change in the extraction mechanism upon changing the aqueous phase acidity was shown by others as well [32,59,60]. However, for NpO_2^{2+}, the extraction takes place by a 'solvation' mechanism only up to 3 M HNO_3 and later decreases due to proton extraction by both the ligands (Fig. 3). Both Np^{4+} and NpO_2^{2+} show a 'solvation' mechanism for the extraction with tributyl phosphate (TBP) dissolved in C_8mim•NTf_2 [28], whereas, a 'cation-exchange' mechanism for the extraction of UO_2^{2+} was reported by Gaillard et al. [32] for TBP dissolved in C_4mim•NTf_2. A 'solvation' mechanism was proposed by Mohapatra et al. for the UO_2^{2+} ion extraction with TOPO (trioctylphosphine oxide) dissolved in C_8mim•NTf_2. Ansari et al. reported a 'cation-exchange' mechanism being operative for the extraction of NpO_2^{2+} ion, and a solvation mechanism for Np^{4+} ion extraction with TODGA in C_8mim•NTf_2 [61]. The formation of the cationic $[Pu(NO_3)(CMPO)_x]^{3+}$ species was reported for the extraction of Pu^{4+} ions using CMPO (octyl(phenyl)-*N,N*-diisobutylcarba moylmethylphosphine oxide) in C_8mim•PF_6 [62]. The difference in the extraction mechanism for the tetra- and hexavalent ions with DGA-functionalized ligands along with TODGA and T2EHDGA (*N,N,N′,N′*-tetra-2-ethylhexyl diglycolamide) was also observed by others [55,63,64]. The D-values of Np^{4+} ion in C_8mim•NTf_2 are lower than those reported in a 95% *n*-dodecane + 5% isodecanol mixture (Table 1) due to the difference in the extraction mechanism and/or solvation of the extracted complex in the two solvents [42].

The sharp decrease in the extraction of the Np^{4+} ion up to 2 M HNO_3 suggests a 'cation-exchange' mechanism being operative for the metal ion extraction by both the ligands in the present system, whereas the extraction get dominated by either a 'solvation' or an 'anion-exchange' mechanism at > 2 M HNO_3. The cation-exchange mechanism with decreasing Np^{4+} ion extraction with acidity up to 2 M HNO_3 can be given by eq. 1. This type of extraction mechanism involving exchange of either H^+ or $C_n$mim$^+$ (n: 4, 6,

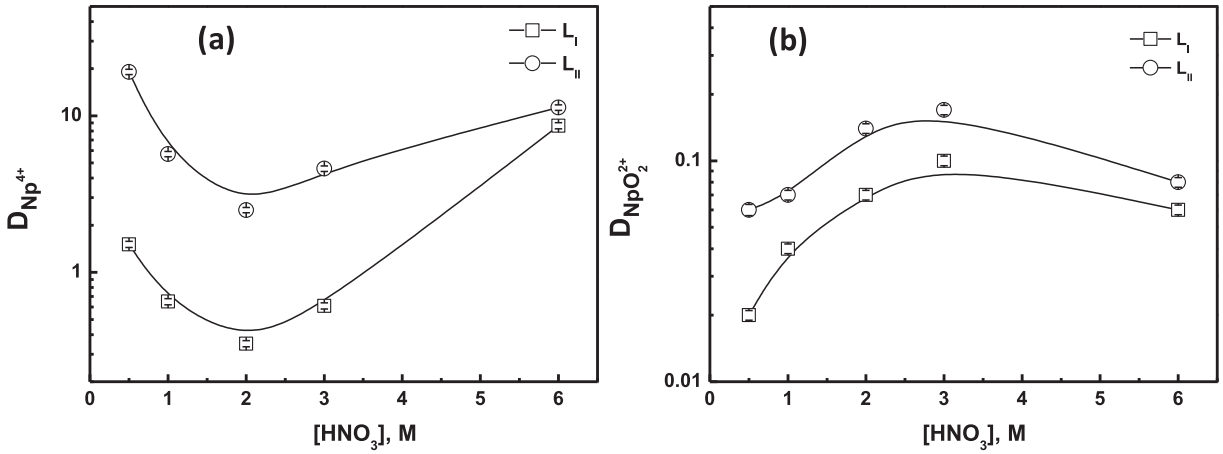

Fig. 3. Extraction of (a) Np^{4+} and (b) NpO_2^{2+} with varying fee acidity using [$\mathbf{L_I}$]: 5 × 10^{-4} M and [$\mathbf{L_{II}}$]: 1 × 10^{-4} M dissolved in C_8mim•NTf_2; T: 298 K.

Table 1
Distribution ratio of Np^{4+} and NpO_2^{2+} by L_I and $\mathbf{L_{II}}$ dissolved in 95% *n*-dodecane + 5% isodecanol and C_8mim•NTf_2 at 3 M HNO_3.

Ligand	95% *n*-dodecane + 5% isodecanol		C_8mim.NTf_2	
	Np^{4+}	NpO_2^{2+}	Np^{4+}	NpO_2^{2+}
$\mathbf{L_I}$	42.7 ± 4.1[a,b]	–[c]	0.6 ± 0.02[d,f]	0.10[d,f]
$\mathbf{L_{II}}$	163 ± 11[a,b]	–[c]	4.6 ± 0.18[e,f]	0.17[e,f]

[a]Ligand concentration: 1×10^{-3} M; [b]Ref [42]; [c]Not reported; [d]-Ligand concentration: 5×10^{-4} M; [e]Ligand concentration: 1×10^{-4} M; [f]Present work.

8, 10) individually or both was also suggested by different authors for the extraction of UO_2^{2+} from ionic liquid ($C_n$mim•NTf_2; n: 4,6,8,10) media using TBP, malonamide, etc.[65–68].

Cation-exchange mechanism:

$$Np^{4+}_{(aq)} + aNO^{-}_{3\,(aq)} + bL_{(IL)} + cH^{+}_{(IL)} + (4-a-c)C_8mim^{+}_{(IL)} \times \overset{K_{ex}^{Np^{4+}}}{\Longleftrightarrow} [Np(NO_3)_a.bL]^{(4-a)+}_{(IL)} + cH^{+}_{(aq)} + (4-a-c)C_8mim^{+}_{(aq)}\ (for\ a<4) \quad (1)$$

The mechanism for Np^{4+} ion extraction beyond 2 M HNO_3 may be due to the anion-exchange (eq. 2) or solvation mechanism (eq. (3)). The possibility of anion-exchange mechanism is low as it requires > 4 nitrate ions along with 'b' number of the ligand, which is difficult due to steric reasons and hence, most plausible mechanism may be solvation mechanism given by eq. (3).

Anion-exchange mechanism:

$$Np^{4+}_{(aq)} + aNO^{-}_{3\,(aq)} + bL_{(IL)} + (4-a)NTf^{-}_{2(IL)} \times \overset{K_{ex}^{Np^{4+}}}{\Longleftrightarrow} [Np(NO_3)_a.bL]^{(4-a)}_{(IL)} + (4-a)NTf^{-}_{2(aq)}\ (for\ a\ >4) \quad (2)$$

Solvation mechanism:

$$Np^{4+}_{(aq)} + 4NO^{-}_{3\,(aq)} + bL_{(IL)} \overset{K_{ex}^{Np^{4+}}}{\Longleftrightarrow} [Np(NO_3)_4.bL]_{(IL)} \quad (3)$$

The extraction profile of NpO_2^{2+} is very much like the extraction of hexavalent ions in the molecular diluents, where the initial increase in the extraction of NpO_2^{2+} is due to the solvation mechanism (up to 3 M HNO_3) and the subsequent decrease is due to the competition between the H^+ and NpO_2^{2+} for both the ligands.

3.3. Speciation of neptunium extracted species in RTIL

The difference in the extraction mechanism of Np^{4+} and NpO_2^{2+} by ligands $\mathbf{L_I}$ and $\mathbf{L_{II}}$ points to a difference in the speciation of the extracted species. The 'cation-exchange' mechanism suggests the formation of cationic species *i.e.*, $Np(NO_3)_a.bL^{(4-a)+}$ (a < 4), whereas the formation of neutral extracted species *i.e.*, $NpO_2(NO_3)_a.bL$ (a = 2), can be considered for the extraction of NpO_2^{2+} in the present system.

The values of 'a' and 'b' were determined as per the following discussion. The general equilibrium reaction for Np^{4+} and NpO_2^{2+} extraction with L ($\mathbf{L_I}$/$\mathbf{L_{II}}$) in C_8mim•NTf_2 can be written as eqs. (1)–(3) for Np^{4+} ion and eq. (4) for the NpO_2^{2+} ion. The solvation mechanism for NpO_2^{2+} is given as:

$$NpO^{2+}_{2(aq)} + bL_{(IL)} + aNO^{-}_{3\,(aq)} \overset{K_{ex}^{NpO_2^{2+}}}{\Longleftrightarrow} [NpO_2.(NO_3)_a]bL_{(IL)} \quad (4)$$

In the equations $L_{(IL)}$ is 'free' L ($\mathbf{L_I}$ or $\mathbf{L_{II}}$) and $\boldsymbol{K_{ex}^{Np^{4+}}}$ and $\boldsymbol{K_{ex}^{NpO_2^{2+}}}$ are the two-phase extraction equilibrium constants for Np^{4+} and NpO_2^{2+} extraction, respectively. The subscripts 'IL' and 'aq' indicate the species present in the C_8mim•NTf_2 and the aqueous phases, respectively.

The steady increase in $\boldsymbol{D_{NpO_2^{2+}}}$ with the aqueous feed acidity indicates a 'solvation' mechanism of extraction and the extraction equilibrium constant for this can be given by Eq. (5):

$$K_{ex}^{NpO_2^{2+}} = \frac{[NpO_2.(NO_3)_a]\cdot bL_{(IL)}}{\left[NpO^{2+}_{2(aq)}\right][L_{(IL)}][NO^{-}_{3(aq)}]\gamma_{NP}(VI)\gamma^{a}_{NO_3}\gamma^{b}_{L}} \quad (5)$$

where the square brackets and γ represent the concentration and activity coefficient of the given species, respectively. With the assumption that the γ for different species remains unity for given concentration of NO_3^- and L, we can rewrite eq. (5) as eq. (6).

$$K_{ex}^{NpO_2^{2+}} = \frac{[NpO_2.(NO_3)_a]\cdot bL_{(IL)}}{\left[NpO^{2+}_{2(aq)}\right][L_{(IL)}][NO^{-}_{3\,(aq)}]} \quad (6)$$

After a few simple mathematical manipulations and approximations, eq. 7 can be derived from eq. (6).

$$Log\ D_{NpO_2^{2+}} = Log\ K_{ex}^{NpO_2^{2+}} + a\ Log[NO^{-}_{3}]_{(aq)} + b\ Log[L]_{(IL)} \quad (7)$$

Where $D_{NpO_2^{2+}}$ is defined as

$$D_{NpO_2^{2+}} = \frac{[NpO_2.(NO_3)_a]\cdot bL_{(IL)}}{\left[NpO^{2+}_{2(aq)}\right]} \quad (8)$$

Eq. (7) gives linear dependence of log $\boldsymbol{D_{NpO_2^{2+}}}$ with the NO_3^- and L concentrations at a particular temperature. A similar mathematical treatment for the extraction of Np^{4+} can also be derived and used for the determination of the nitrate and ligand dependence governing its 'cation-exchange' mechanism. All the extraction experiments for the determination of the stoichiometry of extracted Np^{4+} or NpO_2^{2+} complex in C_8mim•NTf_2 were carried out at 298 K. The stoichiometry of the extracted Np^{4+} and NpO_2^{2+} complexes in the C_8mim•NTf_2 phase can be calculated if the values of 'a' and 'b' are known from eqs. (1) and (2). These values can be easily determined by obtaining the D_{Np} values at varying nitrate concentrations at a fixed ligand concentration and *vice versa*.

To get the value of 'b' for extraction of Np^{4+} or NpO_2^{2+} with L, the concentration of the ligands ($\mathbf{L_I}$ or $\mathbf{L_{II}}$) was varied at a fixed acidity (0.5 M HNO_3 for Np^{4+} and 3 M HNO_3 for NpO_2^{2+}) and the *D*-values of Np^{4+} and NpO_2^{2+} were determined. The nitrate variation experiments were also performed under similar conditions at a fixed ligand concentration.

For the slope analysis in the ligand variation studies, the equilibrium [L_{free}] was assumed to be equal to the initial [L] due to the very small concentrations of Np used in the present study ([Np^{4+} or NpO_2^{2+}]: 10^{-12} M). The log $\boldsymbol{D_{Np^{4+}}}$ *vs* log [L] (L: $\mathbf{L_I}$ / $\mathbf{L_{II}}$) curve gives slope values of 0.95 ± 0.07 and 0.97 ± 0.06 for $\mathbf{L_I}$ and $\mathbf{L_{II}}$, respectively,(Fig. 4) suggesting the involvement of one ligand in the extracted tetravalent species. However, from the log $\boldsymbol{D_{NpO_2^{2+}}}$ *vs* log [L] (L: $\mathbf{L_I}$ / $\mathbf{L_{II}}$) plots, the slope values are 0.66 ± 0.06 and 0.78 ± 0.02 for $\mathbf{L_I}$ and $\mathbf{L_{II}}$, respectively (Fig. 4).

The smaller slope value in case of NpO_2^{2+} may be due to some redox fluctuation during the extraction cycle. Nitrate variation studies were carried out to determine the value of 'a' for the extraction of Np^{4+} and NpO_2^{2+} at a fixed concentration of L (L: $\mathbf{L_I}$ or $\mathbf{L_{II}}$). The nitrate complexation correction for the aqueous Np^{4+}-nitrate complexation was done [29,37] before the slope analysis and all the corrected values were used for it. The nitrate variation studies suggested involvement of one nitrate in the extraction of Np^{4+} (Fig. 5) giving rise to cationic species in both the ligand systems, whereas, for NpO_2^{2+}, involvement of two nitrate ions (Fig. 5) clearly follows from the slope analysis experiments pointing to the extraction of neutral complexes. The ligand and nitrate variation studies suggest formation of $Np(NO_3)]^{3+}$•L and $NpO_2(NO_3)_2$•L (L: $\mathbf{L_I}$ or $\mathbf{L_{II}}$) species for the extraction of Np^{4+} and NpO_2^{2+} ions, respectively. The slope values for the different systems are given in Table 2. The formation of 1:1 neutral Np-$\mathbf{L_I}$/$\mathbf{L_{II}}$ complexes was also reported in the molecular diluents [42].

3.4. Thermodynamic parameters of extraction

To determine the thermodynamic parameters of the extraction process, the extraction of Np^{4+} and NpO_2^{2+} with 5×10^{-4} M $\mathbf{L_I}$ and 1×10^{-4} M$\mathbf{L_{II}}$ dissolved in C_8mim•NTf_2 was studied at different temperatures. The different concentrations of $\mathbf{L_I}$ and $\mathbf{L_{II}}$ was used to obtain reasonably good D-values in the studied temperature range. The D-values for both Np^{4+} and NpO_2^{2+} decrease with increasing temperature for both the ligand systems suggesting an exothermic nature of the extraction process (Fig. 6). For the thermodynamic parameter calculation, the activity coefficients for all species were assumed to be unity (eq. (5)) due to their very small concentrations ([L]:$\simeq 10^{-4}$ M, [Np]: 10^{-12} M), except for NO_3^- ions. Under the assumption that the activity of NO_3^- ion and **L** remains unchanged and the value of K_{Nit} [29,37] also remains constant in the studied temperature range, the Gibbs-Helmholtz equation and $\Delta G_o = -RT\ln K_{ex}$ were used to calculate enthalpy change (ΔH_o) (eq. (9)) in the extraction of Np^{4+} and NpO_2^{2+} by $\mathbf{L_I}$ and $\mathbf{L_{II}}$ at 3 M HNO_3.

$$\log K'_{ex} = -\frac{\Delta H_0}{2.303RT} \times 1000 + \frac{\Delta S_0}{2.303R} \quad (9)$$

The slope of the straight-line plots of log K_{ex} *vs* $1/T$ can be used to calculate the ΔH_o values (in kJ.mol^{-1}) using eq. (9):

$$\Delta H_0 = -2.303R \times slope \quad (10)$$

where, R is the universal gas constant. The slope values along with the calculated thermodynamic parameters are included in Table 3.

The values of K_{ex} for the extraction of Np^{4+} and NpO_2^{2+} by $\mathbf{L_I}$/$\mathbf{L_{II}}$ were calculated at 3 M HNO_3 using the activity of nitrate ions as 2.78 M, computed at 3 M HNO_3 from the dissociation constant of HNO_3 (K_{diss}: 23) [37]. For the computation of K_{ex}, the value of K_{Nit} was taken as 40.5 and 2.2 for Np^{4+} and NpO_2^{2+} ions, respectively, at 3 M HNO_3 [37,69]. The values of the thermodynamic parameters ΔG_O, ΔH_O and $T\Delta S_O$ together with the K_{ex} values are listed in Table 3.

In the solvent extraction process, the overall enthalpy change (ΔH_O) during the extraction of a metal ion (M^{n+}) results from the sum of the enthalpies of the different processes, such as the energy required to overcome the hydration of M^{n+}(ΔH_W), complexation of M^{n+} with **L** (ΔH_C) and dissolution of the extracted complex [M$(NO_3)_a]^{+(n-a)}$•bL complex into the organic solvent (ΔH_D) [70,71]. The other secondary or outer interactions of liquid–liquid extraction such as solvent restructuring, ligand de-solvation and aggregation, solvation energy of ML complex in organic phase, etc., also play an important role in deciding overall thermodynamic feasibility of the extraction process, but are omitted presently to make the discussion simple.

The overall magnitude and sign of ΔH_0 depends on the sum of the contributions of all these enthalpies, *i.e.*, ΔH_W, ΔH_C and ΔH_D, as given in eq. (11)[70,71].

$$H_o = \Delta H_w + \Delta H_c + \Delta H_D \quad (11)$$

Similarly, all the steps in the solvent extraction process have associated entropy factors and the combination of the two *i.e.*, the enthalpy change and the entropy change in each step, decides the free energy of the individual steps. The summation of all these free energy terms results in the overall free energy (ΔG_o) of the extraction process.

Although the ΔH_W term is generally positive (endothermic process) as energy is required for the dehydration of a M^{n+}, the overall extent of the energy requirements depends on the ionic potential of the involved metal ions. The dehydration of Np^{4+} requires more energy than that of NpO_2^{2+} due to the higher ionic potential of the former. The more positive value of ΔH_W for Np^{4+} may get compensated by the higher negative value of the ΔH_C compared to NpO_2^{2+}. The ΔH_D values for the dissolution of the neutral and cationic complexes in ionic liquid may be different as the two complexes interact in different ways with the C_8mim•NTf_2. The overall Gibbs free energy (ΔG_o) for Np^{4+} extraction with both the ligands was found to be more negative than that of NpO_2^{2+} extraction, primarily due to the higher extraction equilibrium constant of the former (Table 3). The higher value of ΔG_o suggests a stronger interaction

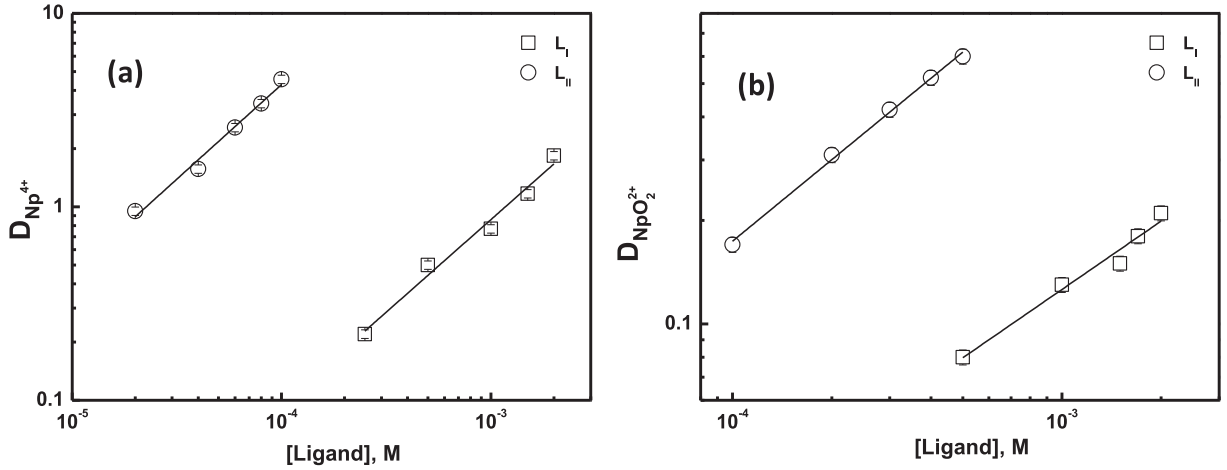

Fig. 4. Extraction of (a) Np^{4+} at 0.5 M HNO_3 and (b) NpO_2^{2+} at 3 M HNO_3 as a function of varying ligand $\mathbf{L_I}$ and $\mathbf{L_{II}}$ concentrations in C_8mim•NTf_2; T: 298 K.

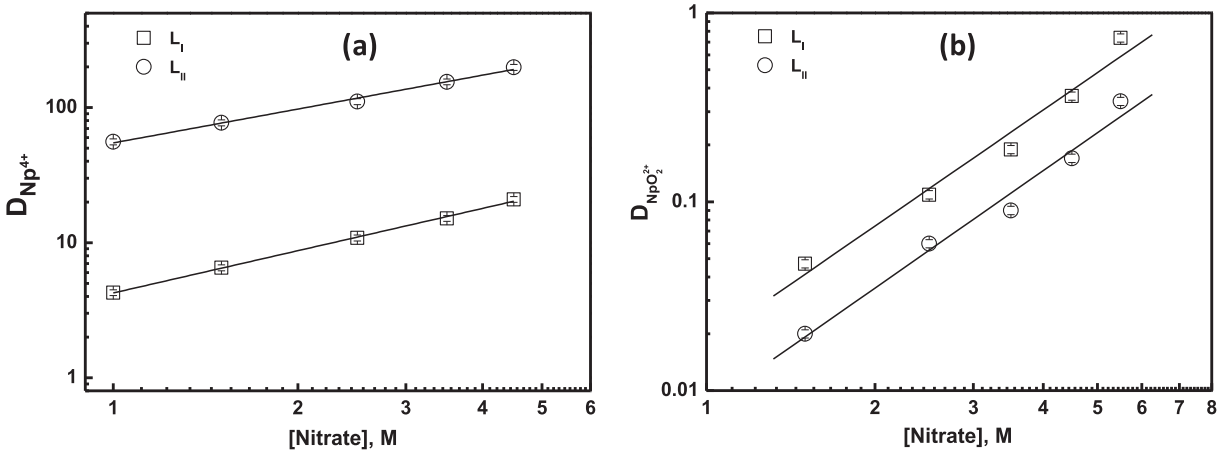

Fig. 5. Extraction of (a) Np^{4+} and (b) NpO_2^{2+} as a function of varying nitrate concentration using [$\mathbf{L_I}$]:5 × 10^{-4} M and [$\mathbf{L_{II}}$]: 1 × 10^{-4} M dissolved in C_8mim•NTf_2; T: 298 K.

Table 2
Stoichiometry of the Np^{4+} and NpO_2^{2+} extracted complexes with L (L: $\mathbf{L_I}$/$\mathbf{L_{II}}$) dissolved in C_8mim•NTf_2.

Ligand	Metal ion		
	Np^{4+}		
	Nitrate	Ligand	Species
$\mathbf{L_I}$	1.03 ± 0.02	0.95 ± 0.07	$Np(NO_3)]^{3+}.\mathbf{L_I}$
$\mathbf{L_{II}}$	0.83 ± 0.03	0.97 ± 0.06	$Np(NO_3)]^{3+}.\mathbf{L_{II}}$
	NpO_2^{2+}		
	Nitrate	Ligand	
$\mathbf{L_I}$	2.04 ± 0.19	0.66 ± 0.06	$NpO_2(NO_3)_2.\mathbf{L_I}$
$\mathbf{L_{II}}$	2.06 ± 0.17	0.78 ± 0.02	$NpO_2(NO_3)_2.\mathbf{L_{II}}$

of Np^{4+} with both ligands and a better solubility of the cationic extracted complex in C_8mim•NTf_2 compared to those of NpO_2^{2+}.

The enthalpy contribution to overall ΔG_o is small for the extraction of the Np^{4+} ion as compared to that of the NpO_2^{2+} ion for both the ligands, whereas the ΔS_o contribution remains in a similar range. Since the overall size of the extracted complex for Np^{4+} and NpO_2^{2+} is decided by the coordinated ligands as other coordinating ions such as water or nitrate are very small compared to the size of $\mathbf{L_I}$ and $\mathbf{L_{II}}$. The contribution of ΔH_D can be assumed in the similar range (except the contribution from ionic interactions with Np^{4+} cationic species and C_8mim•NTf_2) and the other enthalpy changes, *i.e.*, $\Delta H_W + \Delta H_C$, play a deciding role in the overall enthalpy change.

For both NpO_2^{2+} and Np^{4+}, the required positive ΔH_W is compensated by the negative ΔH_C, but the intrinsic play between the two decides the resultant enthalpy. For Np^{4+}, ΔH_W is high, but the compensated ΔH_C is also more as it forms a strong complex with both the ligands, whereas for NpO_2^{2+}, the ΔH_W ($\Delta H_W(NpO_2^{2+})$ < ΔH_W (Np^{4+})) compensation by ΔH_C may not be very effective due to weak interaction with both ligands due to its smaller ionic potential and steric factors (due to the linear shape of the cation). The calculated thermodynamic parameters indicate that the overall extraction equilibria are entropy driven with a higher negative free energy for the extraction of Np^{4+} ion being higher than that of the NpO_2^{2+} ion in the case of both the ligands.

The higher contribution of ΔS_o in the extraction process may be attributed to the release of coordinated H_2O from primary and secondary hydration shells before complexation and the 'distortion' created in the ionic liquid phase by dissolution of the extracted complex. The absorption, cyclic voltammetry and theoretical studies were also done to get further insight into the structural and bonding aspects.

3.5. Spectrophotometric studies

Visible-Near infra-red (vis-NIR) spectra of the extracted Np^{4+} complexes with $\mathbf{L_I}$/$\mathbf{L_{II}}$ dissolved in C_8mim•NTf_2 were recorded in the wavelength range of 600–1100 nm (Fig. 7). In general, the vis-NIR spectra of the Np^{4+}_{aq} show several f-f transitions in the region 600–1100 nm at 0.5 M HNO_3 [72]. The f-f transitions for Np^{4+}(f^3 sys-

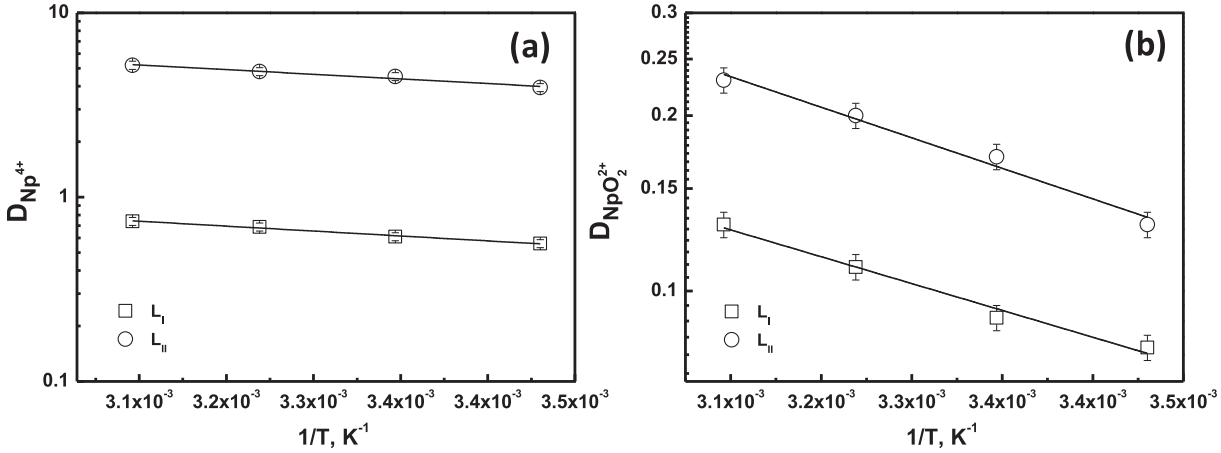

Fig. 6. Effect of temperature on the extraction of (a) Np^{4+} and (b) NpO_2^{2+} with $\mathbf{L_I}$ and $\mathbf{L_{II}}$ at 3 M HNO_3, [L_I]: 5 × 10^{-4} M and [$\mathbf{L_{II}}$]: 1 × 10^{-4} M.

Table 3
Thermodynamic parameters (kJ/mol) for the extraction of Np^{4+} and NpO_2^{2+} by the $\mathbf{L_I}$ and $\mathbf{L_{II}}$ dissolved in $C_8mim{\bullet}NTf_2$ at 298 K.

Ligand	Metal ion				
	Np^{4+}				
	ΔG_o	ΔH_o	ΔS_o	$T\Delta S_o$	log K_{ex}
$\mathbf{L_I}$	−24.2(±1.2)	7.3(±0.4)	0.11(±0.01)	31.5(±1.6)	4.25(0.21)
$\mathbf{L_{II}}$	−33.2(±1.6)	6.9(±0.3)	0.13(±0.01)	40.1(±2.1)	5.81(0.29)
	NpO_2^{2+}				
$\mathbf{L_I}$	−9.4(±0.4)	12.6(±0.6)	0.08(±0.01)	22.1(±1.1)	1.65(0.08)
$\mathbf{L_{II}}$	−14.9(±0.7)	14.32(±0.5)	0.10(±0.01)	29.3(±1.4)	2.63(0.13)

tem) are mainly arising from the $^4I_{9/2}$ state to the higher $^4I_{11/2}$, $^4I_{13/2}$, $^2G_{7/2}$, $^2H_{9/2}$, etc., states [73,74].

The vis-NIR spectra of the extracted Np-$\mathbf{L_I}$ and Np-$\mathbf{L_{II}}$ complexes look similar (Fig. 7) in $C_8mim.NTf_2$ suggesting a similar ligand coordination environment around the Np^{4+} ion in both systems. This result is in line with the theoretical studies (*vide infra*) where the optimized structure of the Np-$\mathbf{L_I}$ and Np-$\mathbf{L_{II}}$ complexes are nine-coordinated in both cases for a 1:1 Np-L complex. The formation of a similar stoichiometry complex may not always have similar local coordination environments as seen by Verma et al. for the Np extraction with a DGA-based dendrimer in RTIL [29].

The relative shift in the peak position of Np in the vis-NIR spectra in the regions 650–750 nm and 950–990 nm can be used to get some information about the relative stability of the Np complex with the ligand in a given medium [75]. For the present system, the relative f-f transition positions for the Np-$\mathbf{L_I}$ and Np-$\mathbf{L_{II}}$ complexes are very close, suggesting similar complexation strength of $\mathbf{L_I}$ and $\mathbf{L_{II}}$ for Np^{4+}. This looks chemically logical, also as the main coordinating sites are very much similar in the two ligands.

3.6. Cyclic voltammetry studies

Information about the relative stability of the Np-$\mathbf{L_I}$ and Np-$\mathbf{L_{II}}$ complexes in RTIL can also be gained by cyclic voltammetry (CV). These studies were done to get some more insight about the electron-donating tendency of the ligating atom in the Np-L complexes or the strength of complexation of $\mathbf{L_I}$ and $\mathbf{L_{II}}$ with Np^{4+}. The extraction of Np^{4+} using $\mathbf{L_I}$ and $\mathbf{L_{II}}$ dissolved in $C_8mim.NTf_2$ was done at 0.5 M HNO_3 to minimize acid uptake by the ligand-$C_8mim.NTf_2$ system (Fig. 8). Extracted HNO_3 can avoid interference with the CV studies and can also shorten the electrochemical window primarily due to the extracted water molecules along with the HNO_3 (Fig. 8). Organic extracts of 0.14×10^{-3} M Np^{4+} in $\mathbf{L_I}$, and 0.70×10^{-3} M Np^{4+} in $\mathbf{L_{II}}$ dissolved in $C_8mim{\bullet}NTf_2$ were taken for CV studies.

The CV of the Np-L extracts in $C_8mim.NTf_2$ along with blank $C_8mim.NTf_2$ and Np in 0.5 M HNO_3 are given in Fig. 9. The CV of the blank (only $C_8min.NTf_2$) did not show any cathodic or anodic peak in the studied range (-1.8 V to + 1.5 V), indicating the absence of any electro active species in the blank. One cathodic and one anodic peak were observed for all Np complexes during the CV scan in the applied potential range of −1.8 to + 1.8 V. The Np^{4+}-Np^{3+} couple in the HNO_3 acid medium shows one electron reduction at + 0.02 V and the corresponding oxidation was seen at 0.27 V (Fig. 9). The observed cathodic peak potentials of the Np-$\mathbf{L_I}$ and Np-$\mathbf{L_{II}}$ complexes are −0.47 V and −0.52 V, respectively. The cathodic peak corresponds to the reduction of a Np^{4+}-L complex into a Np^{3+}-L complex, whereas the corresponding oxidation is indicated by the anodic peak. The higher negative shift in the cathodic peak potential suggests a better complexation or more effective electron donation by the ligand to the metal ion [76,77]. Beside the metal–ligand complexation stability, the overall extraction efficiency of the complex in the organic phase is also affected by other factors, such as hydrophobicity of the metal–ligand complex, phase transfer energy, solvation, etc. [29,71,78]. Although the cathodic peak potential for both the Np-$\mathbf{L_I}$ and Np-$\mathbf{L_{II}}$ are in a similar range (Table 4) (Np-$\mathbf{L_I}$: −0.47 V and Np-$\mathbf{L_{II}}$: −0.52 V), extraction of Np-$\mathbf{L_{II}}$ is more, probably due to the higher lipophilicity of the extracted complex.

A scan rate variation experiment was carried out at different temperatures to gain information about both the diffusion coefficient and the associated activation energy of the Np-L (L = $\mathbf{L_I}$, $\mathbf{L_{II}}$) complexes in $C_8mim{\bullet}NTf_2$. The diffusion coefficient (D_0) of the Np-L species was calculated using the Randles-Sevcik equation,

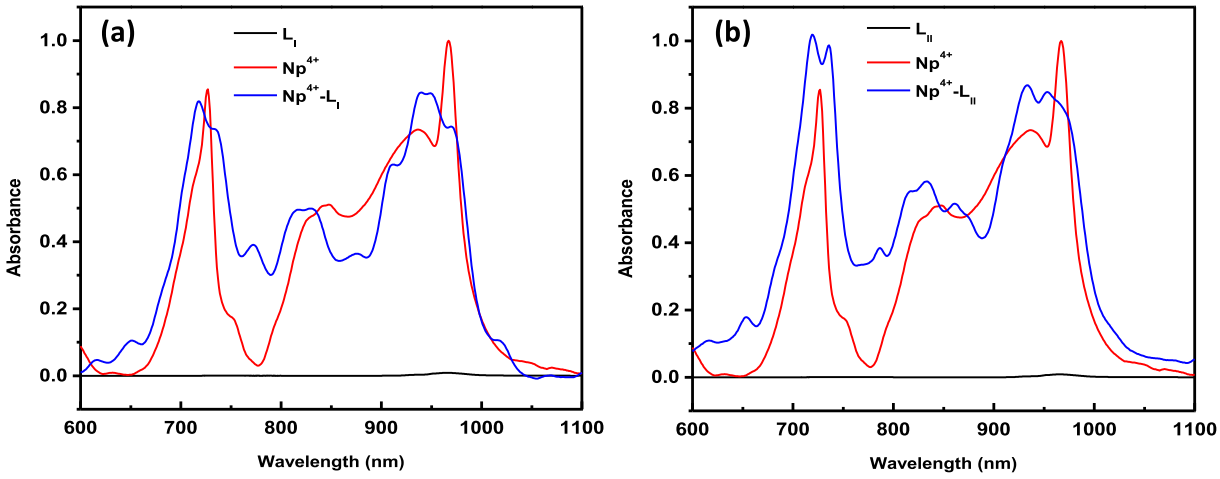

Fig. 7. Vis-NIR absorption spectra of (a) Np^{4+}, $\mathbf{L_I}$, extracted Np^{4+} -$\mathbf{L_I}$ complexes and (b) Np^{4+}, $\mathbf{L_{II}}$ and extracted Np^{4+} -$\mathbf{L_{II}}$ complexes dissolved in $C_8mim.NTf_2$, [Np]: 1.2 mM; T: 298 K.

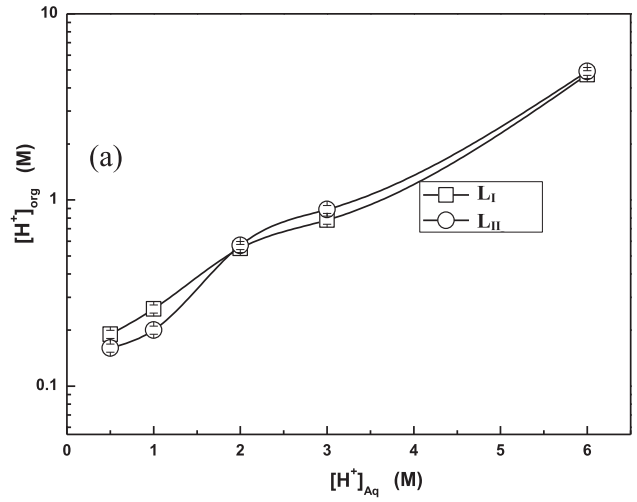

Fig. 8. Acid uptake by ligands, $\mathbf{L_I}$ and $\mathbf{L_{II}}$ dissolved in C_8mim•NTf_2 at different nitric acid concentrations, T: 298 K.

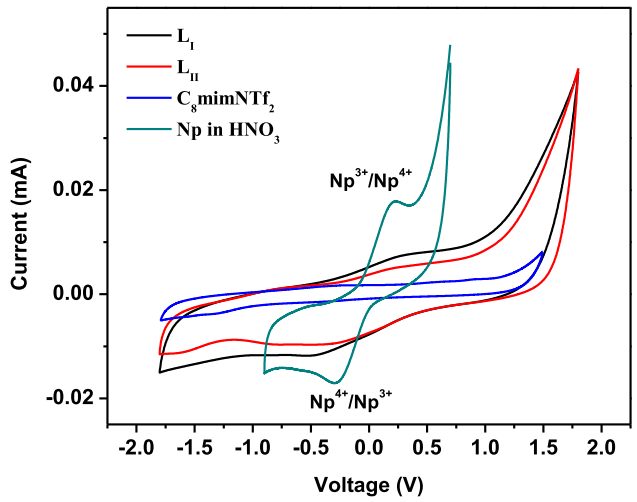

Fig. 9. CV studies of Np in 0.5 M HNO_3 and Np^{4+} extract with $\mathbf{L_I}$ and $\mathbf{L_{II}}$ dissolved in C_8mimNTf_2. Scan rate: 0.1 Vs^{-1}, T: 298 K.

Table 4
Cathodic peak potentials of aqueous Np (at 0.5 M HNO_3) and extracted Np-L complexes in C_8mim•NTf_2. Scan rate: 0.1 V s^{-1}.

Complex	$E_{p,c}$(Volt)
Np[a]	+0.02
Np-$\mathbf{L_I}$[b]	−0.47
Np-$\mathbf{L_{II}}$[c]	−0.52

[Np]: [a] 1.26 mM, [b] 0.14×10^{-3} M, [c] 0.70×10^{-3} M.

where the cathodic peak current of the Np^{4+}-Np^{3+} reduction couple was plotted against the square root of the scan rate to get a straight line (eq. (12)).

$$i_c^p = 0.496.nFCAD_0^{\frac{1}{2}}\left(\frac{\alpha n_\alpha F\upsilon}{RT}\right)^{\frac{1}{2}} \quad (12)$$

In eq. (12) F is the Faraday constant, n is the number of electrons involved, A is the area of the electrode (0.07 cm^2), D_0 is the diffusion coefficient (cm^2 s^{-1}), C is the bulk concentration of the Np species (mol cm^{-3}), υ is the scan rate (V s^{-1}), R is the gas constant, and T is the temperature in K. α is the charge transfer coefficient, n_α is the number of electrons transferred in the rate-determining step. The term αn_α can be deduced from the CV scan using eq. (13).

$$\left|E_p^c - E_{\frac{p}{2}}^c\right| = \frac{1.857RT}{\alpha n_\alpha F} \quad (13)$$

Where $E_{p/2}^c$ is the half peak potential. The calculated value of αn_α was found to be 0.32 and 0.25 with Np-$\mathbf{L_I}$ and Np-$\mathbf{L_{II}}$, respectively, at 298 K for a scan rate of 0.1 V s^{-1}. The D_o-value of Np-$\mathbf{L_I}$ and Np-$\mathbf{L_{II}}$ was found to be 4.35×10^{-6} and 5.83×10^{-7} cm^2 s^{-1}, respectively, at 298 K. The lower diffusion coefficient obtained in the case of $\mathbf{L_{II}}$ suggests a larger size of the Np-$\mathbf{L_{II}}$ complex, which is evident due to the larger size of $\mathbf{L_{II}}$ compared to $\mathbf{L_I}$.

The diffusion coefficient (D_o) of an electrochemical species is also related to temperature by the Arrhenius equation shown in eq. (14):

$$D_0 = A.\exp(-\frac{E_a}{RT}) \quad (14)$$

Where A is the pre-exponential factor and E_a is the activation energy. The plot of ln D_0 against 1/T gives a straight line and from its slope (Fig. 10), the activation energy for the diffusion of the Np-L complex can be calculated. The activation energy of Np-$\mathbf{L_I}$ and Np-$\mathbf{L_{II}}$ diffusion in C_8mim.NTf_2 was found to be 28.05 ± 1.28 and 21.93 ± 2.24 kJ/mol, respectively, at 298 K suggesting facile diffusion of the former complex as compared to the latter.

3.7. DFT studies on Np^{4+} and NpO_2^{2+} complexes of L_I and L_{II}

Solvent extraction studies indicated the formation of a 1:1 complex of Np^{4+} with $\mathbf{L_I}$ where the presence of one nitrate ion is noticed from the nitrate ion variation study. The geometry of this complex was, therefore, optimized considering this information. In the optimized structure, Np^{4+} was encapsulated by the three DGA arms of one ligand molecule. Two different types of amidic oxygen atoms (O_{amide}) are observed in this class of ligands, one is far from the azacrown ring ($O_{amide(o)}$) and another one is close to the azacrown ring ($O_{amide(i)}$). Table 5 shows that all the three '$O_{amide(o)}$' atoms coordinate to the Np^{4+} ion in its $\mathbf{L_I}$ complex with bond lengths in the range of 2.26–2.35 Å. On the other hand, only

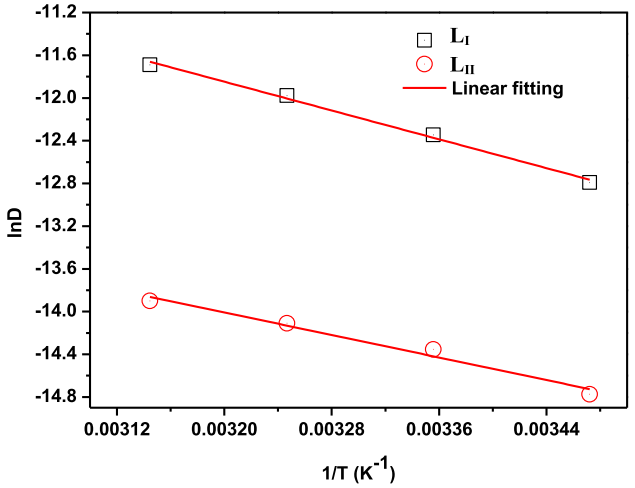

Fig. 10. Arrhenius plot for the diffusion of Np-L (L: $\mathbf{L_I}$ and $\mathbf{L_{II}}$) complexes in C_8mim•NTf_2.

Table 5
Np-O bond distances in different Np complexes of $\mathbf{L_I}$ and $\mathbf{L_{II}}$.

Np-O bond	Neptunium complex			
	Np^{4+}-$\mathbf{L_I}$	Np^{4+}-$\mathbf{L_{II}}$	NpO_2^{2+}-$\mathbf{L_I}$	NpO_2^{2+}-$\mathbf{L_{II}}$
$Np\text{-}O_{amide(o)}$	2.266, 2.268, 2.352	2.304, 2.315, 2.321	2.424	2.317, 2.330, 2.398
$Np\text{-}O_{amide(i)}$	2.362, 4.292, 4.868	2.388, 2.400, 2.633	2.517	–
$Np\text{-}O_{ether}$	2.646, 2.697, 2.772	2.615, 2.750, 4.588	3.757	–
$Np\text{-}O_{NO3}$	2.363, 2.374	2.202	2.474,2.481, 2.495,2.508	2.239, 4.424
$Np\text{-}O_{ax}$	–	–	1.773, 1.774	1.743, 1.752

one of the three '$O_{amide(i)}$' atoms coordinates to the Np^{4+} ion. As expected, a weaker interaction is observed between the Np^{4+} ion and the ethereal oxygen (O_{ether}) atoms of the DGA arms with bond lengths in the range of 2.64–2.77 Å. Np^{4+} was found to be ten-coordinated in its $\mathbf{L_I}$ complex (Fig. 11). On the other hand, in the $\mathbf{L_{II}}$ complex of Np^{4+} only three of the four DGA arms participate in bonding with the Np^{4+} ion and the fourth arm remains completely non interacting (Fig. 11b). NpO_2^{2+} was also extracted as 1:1 complex associated with two nitrate ions. The optimized structures of the NpO_2^{2+} complexes are shown in Fig. 12. In its $\mathbf{L_I}$ complex, only one of the three arms of the ligand coordinates to the metal ion in a bidentate fashion through two amidic oxygen atoms. Two nitrate ions coordinate in bidentate fashion. In the $\mathbf{L_{II}}$ complex of NpO_2^{2+}, however, three DGA arms participate in coordination to the NpO_2^{2+} ions only through one O_{amide} atom of each of the arms. Out of the two nitrate ions, here, only one coordinates in monodentate fashion, whereas the other one remains in the outer sphere. Comparing of the $Np\text{-}O_{ax}$ bond length in the two complexes of NpO_2^{2+}, it is interesting to note that in case of the NpO_2^{2+}-$\mathbf{L_I}$ complex, the $Np\text{-}O_{ax}$ bond lengths are greater than in theNpO_2^{2+}- $\mathbf{L_I}$ complex. This can be attributed to a higher transfer of electron density to the NpO_2^{2+} ion through the equatorial ligands in the NpO_2^{2+}-$\mathbf{L_I}$ complex due to the presence of two nitrate ions. In order to find out the relative complexation ability the interaction energies (ΔE) were compared for the complexation reactions (13) and (14) for Np^{4+} and NpO_2^{2+}, respectively,

$$Np^{4+} + L + NO_3^- \rightleftharpoons NpL(NO_3)^{3+} \quad (15)$$

$$NpO_2^{2+} + L + 2NO_3^- \rightleftharpoons NpO_2L(NO_3)_2 \quad (16)$$

The ΔE values were calculated as the difference between the sum of the product and reactant energies. Table 6 clearly shows that Np^{4+} complexation is much stronger than NpO_2^{2+} complexation in the case of both the ligands, which nicely supports the observed results of the solvent extraction studies, the extraction of Np^{4+} being much higher than that of NpO_2^{2+}. If we compare the complexation of Np in a particular oxidation state, Np^{4+} complexation is stronger with $\mathbf{L_{II}}$ as compared to that with $\mathbf{L_I}$ resulting in significantly higher extraction of Np^{4+} with $\mathbf{L_{II}}$ as compared to $\mathbf{L_I}$. In case of NpO_2^{2+}, on the other hand, the interaction energies are comparable for both ligands. The marginally higher extraction in case of $\mathbf{L_{II}}$ can be explained based on the higher lipophilicity of $\mathbf{L_{II}}$ due to the presence of four DGA arms having each octyl groups.

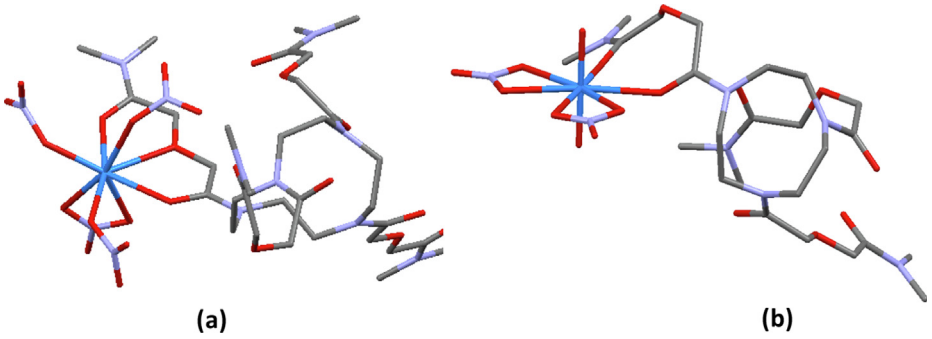

Fig. 11. Optimized structures of Np^{4+} complexes of ligands $\mathbf{L_I}$ and $\mathbf{L_{II}}$.

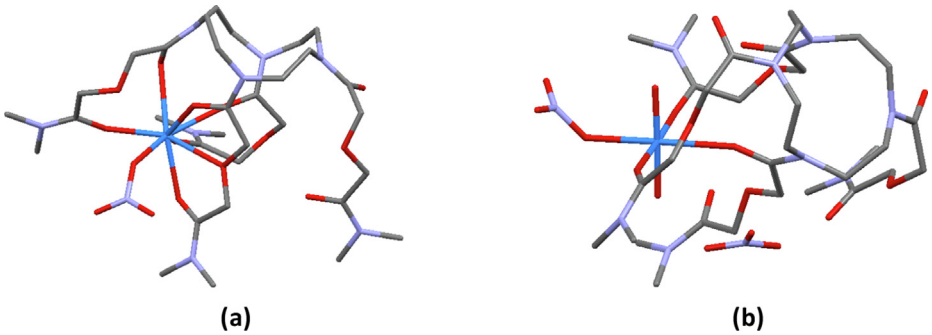

Fig. 12. Optimized structures of NpO_2^{2+} complexes of ligands $\mathbf{L_I}$ and $\mathbf{L_{II}}$.

Table 6
Interaction energies (in eV) in different complexes of Np^{4+} and NpO_2^{2+} formed with ligands $\mathbf{L_I}$ and $\mathbf{L_{II}}$.

Metal ion	Ligand	
	$\mathbf{L_I}$	$\mathbf{L_{II}}$
Np^{4+}	−58.21	−59.83
NpO_2^{2+}	−25.46	−25.14

4. Conclusions

The extraction of Np^{4+} and NpO_2^{2+} was evaluated with two aza-crown ether scaffolds tethered with DGA arms (**LI** and $\mathbf{L_{II}}$) in C_8mim.NTf_2. The extraction of Np^{4+} follows a 'cation-exchange' mechanism with both ligands, whereas NpO_2^{2+} extraction proceeds by the 'solvation' mechanism. The stoichiometry of the extracted NpO_2^{2+} was found to be $NpO_2(NO_3)_2$.L (L: $\mathbf{L_I}$ and $\mathbf{L_{II}}$) in C_8mim•NTf_2, which is similar as in 95% *n*-dodecane + 5% isodecanol [42]. However, the stoichiometry of the extracted Np^{4+} ion complex was the same with respect to the associated ligand molecule in C_8mim•NTf_2 and 95% *n*-dodecane + 5% isodecanol but differs in the coordinated nitrate molecules. The extracted Np^{4+} forms a cationic moiety with only one nitrate ion in C_8mim•NTf_2, whereas a neutral species is reported in 95% *n*-dodecane + 5% isodecanol [42]. The thermodynamic studies show that the extraction process is endothermic in nature. The higher contribution of ΔS_o in the extraction process of Np^{4+} and NpO_2^{2+} with both ligands drives the extraction equilibrium. Although Vis-NIR, CV studies along with the theoretical calculations suggest a similar coordinating ability of $\mathbf{L_I}$ and $\mathbf{L_{II}}$ towards Np^{4+} ion, the higher extraction of Np^{4+} ion by $\mathbf{L_{II}}$, is probably due to the higher lipophilicity of the extracted complex.

The present solvent extraction studies along with the vis-NIR, electrochemical and DFT studies gives an insight into the coordination of Neptunium with DGA-based ligands in the ionic liquid. Further spectroscopic and EXFAS-based studies are needed to better illustrate interaction of the Np with the different ligand systems in the ionic liquid media at the molecular level.

CRediT authorship contribution statement

Rajesh B. Gujar: Data curation. **Parveen K. Verma:** UV-vis spectroscopy, Data curation. **Bholanath Mahanty:** Electrochemistry. **Arunasis Bhattacharyya:** DFT. **Sk. Musharaf Ali:** DFT. **Richard J. M. Egberink:** Synthesis. **Jurriaan Huskens:** Supervision. **Willem Verboom:** Writing – review & editing. **Prasanta K. Mohapatra:** Conceptualization, Visualization, Writing – review & editing.

Data availability

Data will be made available on request.

Declaration of Competing Interest

The authors declare that they have no known competing financial interests or personal relationships that could have appeared to influence the work reported in this paper.

Acknowledgement

One of the authors (SMA) thanks Mr. K.T. Shenoy, Director, Chemical Engineering Group BARC, for his support and encouragement.

References

[1] P.K. Verma, P.K. Mohapatra, Fate of Neptunium in nuclear fuel cycle streams: state-of-the art on separation strategies, Radiochim. Acta (2022). (https://doi.org/10.1515/ract-2022-0008)).
[2] C. Madic, From the reactor to waste disposal: The back-end of the nuclear fuel cycle with emphasis on France, Radiat. Prot. Dosim. 26 (1989) 15–22.
[3] C. Madic, M. Lecomte, P. Baron, B. Boullis, Separation of long-lived radionuclides from high active nuclear waste | Séparation de radionucléides à vie longue des déchets nucléaires haute activité, Comptes Rendus Physique 3 (2002) 797–811.
[4] A. Bhattacharyya, P.K. Verma, P.K. Mohapatra, P.K. Pujari, D. Mehta, C.P. Kaushik, Recent trends and strategies in nuclear Fuel waste management, in: Bhabha Atomic Research Centre, Mumbai - 400 085, Bhabha Atomic Research Centre, 2020.
[5] C. Walther, M.A. Denecke, Actinide colloids and particles of environmental concern, Chem. Rev. 113 (2013) 995–1015.
[6] K. Maher, J.R. Bargar, G.E. Brown Jr, Environmental speciation of actinides, Inorg. Chem. 52 (2013) 3510–3532.
[7] S. Banerjee, P.K. Mohapatra, A. Bhattacharyya, S. Basu, V.K. Manchanda, Extraction of tetravalent neptunium isoxazolonates as their TOPO adducts, Radiochim. Acta 92 (2004) 95–99.
[8] R. Gujar, G. Dhekane, P. Mohapatra, Liquid–liquid extraction of Np^{4+} and Pu^{4+} using several tetra-alkyl substituted diglycolamides, Radiochim. Acta 101 (2013) 719–724.
[9] R.B. Gujar, P.K. Mohapatra, W. Verboom, Extraction of Np^{4+} and Pu^{4+} from nitric acid feeds using three types of tripodal diglycolamide ligands, Sep. Purif. Technol. 247 (2020) 116986.
[10] B. Mahanty, P.K. Mohapatra, A. Leoncini, J. Huskens, W. Verboom, Liquid–liquid extraction and supported liquid membrane transport of Neptunium (IV) across a flat-sheet supported liquid membrane containing a TREN-DGA derivative., Solvent Extr. Ion Exch. 40 (7) (2022) 693–717.
[11] B. Mahanty, A. Bhattacharyya, A.S. Kanekar, P.K. Mohapatra, Selective Separation of Neptunium from an Acidic Feed Containing a Mixture of Actinides Using Dialkylamides, Solvent Extr. Ion Exch. 38 (2020) 290–303.
[12] B. Mahanty, A. Bhattacharyya, P.K. Mohapatra, Separation of neptunium (IV) from actinides by solid phase extraction using a resin containing Aliquat 336, J. Chromatogr. A 1564 (2018) 94–101.
[13] P.K. Mohapatra, P.B. Ruikar, V.K. Manchanda, Separation of neptunium and plutonium from acidic medium using 3-phenyl-4-benzoyl-5-isoxazolone, Radiochim. Acta 90 (2002) 323–327.
[14] R. Gujar, S. Ansari, D. Prabhu, P. Pathak, A. Sengupta, S. Thulasidas, P. Mohapatra, V. Manchanda, Actinide partitioning with a modified TODGA solvent: counter-current extraction studies with simulated high level waste, Solvent Extr. Ion Exch. 30 (2012) 156–170.
[15] R.B. Gujar, G.B. Dhekane, P.K. Mohapatra, Liquid-liquid extraction of Np^{4+} and Pu^{4+} using several tetra-alkyl substituted diglycolamides, Radiochim. Acta 101 (2013) 719–724.
[16] R.B. Gujar, P.K. Verma, P.K. Mohapatra, M. Iqbal, J. Huskens, W. Verboom, Extraction of tetra- and hexavalent actinide ions from nitric acid solutions using some diglycolamide functionalized calix[4]arenes, Radiochim. Acta 109 (2021) 167–176.
[17] S.A. Ansari, P.K. Mohapatra, M. Iqbal, P. Kandwal, J. Huskens, W. Verboom, Novel diglycolamide-functionalized calix[4]arenes for actinide extraction and supported liquid membrane studies: Role of substituents in the pendent arms and mass transfer modeling, J. Membr. Sci. 430 (2013) 304–311.
[18] A. Leoncini, P.K. Mohapatra, A. Bhattacharyya, D.R. Raut, A. Sengupta, P.K. Verma, N. Tiwari, D. Bhattacharyya, S. Jha, A.M. Wouda, J. Huskens, W. Verboom, Unique selectivity reversal in Am^{3+}–Eu^{3+} extraction in a tripodal TREN-based diglycolamide in ionic liquid: extraction, luminescence, complexation and structural studies, Dalton Trans. 45 (2016) 2476–2484.
[19] B. Mahanty, P.K. Verma, P. Mohapatra, Extraction of Some Actinide Ions from Nitric Acid Feeds Using *N, N*-di-n-hexyloctanamide (DHOA) in an Ionic Liquid, J. Solution Chem. 49 (2020) 763–776.
[20] S.A. Ansari, P. Pathak, P.K. Mohapatra, V.K. Manchanda, Chemistry of diglycolamides: promising extractants for actinide partitioning, Chem. Rev. 112 (2012) 1751–1772.
[21] P.K. Mohapatra, A. Sengupta, M. Iqbal, J. Huskens, S.V. Godbole, W. Verboom, Remarkable acidity independent actinide extraction with a both-side diglycolamide-functionalized calix[4]arene, Dalton Trans. 42 (2013) 8558–8562.
[22] P.K. Mohapatra, Actinide ion extraction using room temperature ionic liquids: opportunities and challenges for nuclear fuel cycle applications, Dalton Trans. 46 (2017) 1730–1747.
[23] Y. Li, X. Dong, J. Yuan, N. Pu, P. Wei, T. Sun, W. Shi, J. Chen, J. Wang, C. Xu, Performance and Mechanism for the Selective Separation of Trivalent Americium from Lanthanides by a Tetradentate Phenanthroline Ligand in Ionic Liquid, Inorg. Chem. 59 (2020) 3905–3911.
[24] Y. Li, X. Yang, P. Ren, T. Sun, W. Shi, J. Wang, J. Chen, C. Xu, Substituent Effect on the Selective Separation and Complexation of Trivalent Americium and Lanthanides by N, O-Hybrid 2,9-Diamide-1,10-phenanthroline Ligands in Ionic Liquid, Inorg. Chem. 60 (2021) 5131–5139.
[25] L. Xu, N. Pu, Y. Li, P. Wei, T. Sun, C. Xiao, J. Chen, C. Xu, Selective Separation and Complexation of Trivalent Actinide and Lanthanide by a Tetradentate Soft-

Hard Donor Ligand: Solvent Extraction, Spectroscopy, and DFT Calculations, Inorg. Chem. 58 (2019) 4420–4430.
[26] L. Xu, N. Pu, G. Ye, C. Xu, J. Chen, X. Zhang, L. Lei, C. Xiao, Unraveling the complexation mechanism of actinide(III) and lanthanide(III) with a new tetradentate phenanthroline-derived phosphonate ligand., Inorg. Chem. Front. 7 (2020) 1726–1740.
[27] X. Dong, Z. Wang, Q. Yan, H. Liu, Y. Guo, H. Cao, J. Chen, C. Xu, Optically "silent" neptunium (V)-nitrate complex in ionic liquid, Chinese Chem. Lett. 33 (2022) 3531–3533.
[28] P.K. Verma, B. Mahanty, R.B. Gujar, P.K. Mohapatra, Neptunium – Tri-n-butyl phosphate complexes in room temperature ionic liquids: Extraction and spectroelectrochemical studies, J. Mol. Liquids 325 (2021).
[29] P.K. Verma, R.B. Gujar, B. Mahanty, A. Leoncini, J. Huskens, W. Verboom, P.K. Mohapatra, Sequestration of tetravalent neptunium from acidic feeds using diglycolamide-functionalized dendrimers in a room temperature ionic liquid: extraction, spectroscopic and electrochemical studies, New J. Chem. 45 (2021) 17951–17959.
[30] P. Verma, B. Mahanty, P. Mohapatra, Solvent extraction studies with monoamides in room temperature ionic liquid: role of medium for tetravalent, hexavalent separation, In: Proceedings of the Fourteenth Biennial DAE-BRNS Symposium on Nuclear and Radiochemistry: Book of Abstracts, 2019.
[31] I. Billard, A. Ouadi, C. Gaillard, Liquid–liquid extraction of actinides, lanthanides, and fission products by use of ionic liquids: from discovery to understanding, Anal. Bioanal. Chem. 400 (2011) 1555–1566.
[32] D.C. Gaillard, M. Boltoeva, I. Billard, S. Georg, V. Mazan, A. Ouadi, D. Ternova, C. Hennig, Insights into the Mechanism of Extraction of Uranium (VI) from Nitric Acid Solution into an Ionic Liquid by using Tri-n-butyl phosphate, Chem. Phys. Chem. (2015) 2653–2662.
[33] M.P. Jensen, T. Yaita, R. Chiarizia, Reverse-micelle formation in the partitioning of trivalent f-element cations by biphasic systems containing a tetraalkyldiglycolamide, Langmuir 23 (2007) 4765–4774.
[34] M. Iqbal, P.K. Mohapatra, S.A. Ansari, J. Huskens, W. Verboom, Preorganization of diglycolamides on the calix[4]arene platform and its effect on the extraction of Am(III)/Eu(III), Tetrahedron 68 (2012) 7840–7847.
[35] D. Jańczewski, D.N. Reinhoudt, W. Verboom, C. Hill, C. Allignol, M.T. Duchesne, Tripodal diglycolamides as highly efficient extractants for f-elements, New J. Chem. 32 (2008) 490–495.
[36] P.K. Verma, R.B. Gujar, S.A. Ansari, S.M. Ali, R.J.M. Egberink, J. Huskens, W. Verboom, P.K. Mohapatra, Sequestration of Am^{3+} and Eu^{3+} into ionic liquid containing aza-macrocycle based multiple-diglycolamide ligands: Extraction, complexation, luminescence and DFT studies, J. Mol. Liquids 347 (2022).
[37] P.K. Verma, R.B. Gujar, P.K. Mohapatra, S.M. Ali, A. Leoncini, J. Huskens, W. Verboom, Highly efficient diglycolamide-functionalized dendrimers for the sequestration of tetravalent actinides: solvent extraction and theoretical studies, New J. Chem. 45 (2021) 9462–9471.
[38] S.A. Ansari, P.K. Mohapatra, A. Leoncini, J. Huskens, W. Verboom, Benzene-centred tripodal diglycolamides for the sequestration of trivalent actinides: metal ion extraction and luminescence spectroscopic investigations in a room temperature ionic liquid, Dalton Trans. 46 (2017) 11355–11362.
[39] A.B. Patil, P.N. Pathak, V.S. Shinde, P.K. Mohapatra, Synthesis and Evaluation of N, N′-dimethyl-N, N′-dicyclohexyl-Malonamide (DMDCMA) as an Extractant for Actinides, Sep. Sci. Technol. 49 (2014) 2927–2932.
[40] A. Sengupta, P.K. Mohapatra, M. Iqbal, J. Huskens, W. Verboom, A diglycolamide-functionalized task specific ionic liquid (TSIL) for actinide extraction: Solvent extraction, thermodynamics and radiolytic stability studies, Sep. Purif. Technol. 118 (2013) 264–270.
[41] S.A. Ansari, P.K. Mohapatra, A. Leoncini, S.M. Ali, A. Singhadeb, J. Huskens, W. Verboom, Unusual extraction of trivalent f-cations using diglycolamide dendrimers in a room temperature ionic liquid: extraction, spectroscopic and DFT studies, Dalton Trans. 46 (2017) 16541–16550.
[42] S.A. Ansari, A. Bhattacharyya, P.K. Mohapatra, R.J.M. Egberink, J. Huskens, W. Verboom, Evaluation of two aza-crown ether-based multiple diglycolamide-containing ligands for complexation with the tetravalent actinide ions Np^{4+} and Pu^{4+}: extraction and DFT studies, RSC Adv. 9 (2019) 31928–31935.
[43] A. Bhattacharyya, A. Leoncini, R.J.M. Egberink, P.K. Mohapatra, P.K. Verma, A.S. Kanekar, A.K. Yadav, S.N. Jha, D. Bhattacharyya, J. Huskens, W. Verboom, First Report on the Complexation of Actinides and Lanthanides Using 2,2′,2″-(((1,4,7-Triazonane-1,4,7-triyl)tris(2-oxoethane-2,1-diyl)) tris(oxy)) tris(*N*, N-dioctylacetamide): Synthesis, Extraction, Luminescence, EXAFS, and DFT Studies, Inorg. Chem. 57 (2018) 12987–12998.
[44] M.J. Earle, C.M. Gordon, N.V. Plechkova, K.R. Seddon, T. Welton, Decolorization of ionic liquids for spectroscopy, Anal. Chem. 79 (2007) 758–764.
[45] R.B. Gujar, P.K. Verma, B. Mahanty, S.A. Ansari, D. Goswami, P.K. Mohapatra, Comparative evaluation of extraction of tetra- and hexa-valent neptunium ions by CMPO in a room temperature ionic liquid, Sep. Sci. Technol. 55 (2020) 2560–2569.
[46] J.N. Mathur, M.S. Murali, M.V. Balarama Krishna, R.H. Iyer, R.R. Chitnis, P.K. Wattal, T.K. Theyyunni, A. Ramanujam, P.S. Dhami, V. Gopalakrishnan, Recovery of Neptunium from Highly Radioactive Waste Solutions of Purex Origin Using Tributyl Phosphate, Sep. Sci. Technol. 31 (1996) 2045–2063.
[47] R. Ahlrichs, M. Bär, M. Häser, H. Horn, C. Kölmel, Electronic structure calculations on workstation computers: The program system turbomole, Chem. Phys. Lett. 162 (1989) 165–169.
[48] O. Treutler, R. Ahlrichs, Efficient molecular numerical integration schemes, J. Chem. Phy. 102 (1995) 346–354.
[49] V. Turbomole, 7.3, A development of University of Karlsruhe and Forschungszentrum Karlsruhe GmbH, 1989–2007, TURBOMOLE GmbH, since, 2010 (2007)..
[50] A.D. Becke, Density-functional exchange-energy approximation with correct asymptotic behavior, Phys. Rev. A 38 (1988) 3098.
[51] J.P. Perdew, Density-functional approximation for the correlation energy of the inhomogeneous electron gas, Phys. Rev. B 33 (1986) 8822.
[52] A.D. Becke, Density-functional thermochemistry. III. The role of exact exchange, J. Chem. Phys. 98 (1993) 5648–5652.
[53] F. Weigend, R. Ahlrichs, Balanced basis sets of split valence, triple zeta valence and quadruple zeta valence quality for H to Rn: Design and assessment of accuracy, Phys. Chem. Chem. Phys. 7 (2005) 3297–3305.
[54] A. Schäfer, C. Huber, R. Ahlrichs, Fully optimized contracted Gaussian basis sets of triple zeta valence quality for atoms Li to Kr, J. Chem. Phys. 100 (1994) 5829–5835.
[55] D.R. Prabhu, D.R. Raut, M.S. Murali, P.K. Mohapatra, Extraction of plutonium (IV) by diglycolamide extractants in room temperature ionic liquids, Radiochim. Acta 105 (2017) 285–293.
[56] P. Pathak, D. Prabhu, N. Kumari, P. Mohapatra, Studies on the extraction of actinides using a solvent containing D2EHiBA in room temperature ionic liquids: unusual extraction of the tetravalent ions, Sep. Sci. Technol. 50 (2015) 373–379.
[57] A.B. Patil, P. Pathak, V.S. Shinde, S.V. Godbole, P.K. Mohapatra, Efficient solvent system containing malonamides in room temperature ionic liquids: Actinide extraction, fluorescence and radiolytic degradation studies, Dalton Trans. 42 (2013) 1519–1529.
[58] A. Sengupta, P.K. Mohapatra, P. Pathak, T.K. Ghanty, W. Verboom, Studies on neptunium complexation with CMPO- and diglycolamide-functionalized ionic liquids: experimental and computational studies, New J. Chem. 41 (2017) 836–844.
[59] I. Billard, Ionic liquids: new hopes for efficient lanthanide/actinide extraction and separation?, in: Handbook on the Physics and Chemistry of Rare Earths, Elsevier, 2013, pp 213–273.
[60] I. Billard, A. Ouadi, E. Jobin, J. Champion, C. Gaillard, S. Georg, Understanding the extraction mechanism in ionic liquids: $UO_2^{2+}/HNO_3/TBP/C_4$-mimTf_2N as a case study, Solvent Extr. Ion Exch. 29 (2011) 577–601.
[61] S.A. Ansari, P.K. Mohapatra, D.R. Raut, Extraction of Np^{4+} and NpO_2^{2+} from Nitric Acid Medium Using TODGA in Room Temperature Ionic Liquids, J. Solution Chem. 47 (2018) 1326–1338.
[62] K. Lohithakshan, S. Aggarwal, Solvent extraction studies of Pu (IV) with CMPO in 1-octyl 3-methyl imidazolium hexa fluorophosphate (C8mimPF6) room temperature ionic liquid (RTIL), Radiochim. Acta 96 (2008) 93–97.
[63] A. Bhattacharyya, P.K. Mohapatra, D.R. Raut, A. Leoncini, J. Huskens, W. Verboom, Unusual Reversal in Pu and U Extraction in an Ionic Liquid Using Two Tripodal Diglycolamide Ligands: Experimental and DFT Studies, Solvent Extr. Ion Exch. 36 (2018) 542–557.
[64] S.A. Ansari, P.K. Mohapatra, D.R. Raut, Extraction of Np^{4+} and NpO_2^{2+} rom Nitric Acid Medium Using TODGA in Room Temperature Ionic Liquids, J. Solution Chem. 47 (2018) 1326–1338.
[65] I. Billard, A. Ouadi, C. Gaillard, Is a universal model to describe liquid–liquid extraction of cations by use of ionic liquids in reach?, Dalton Trans 42 (2013) 6203–6212.
[66] I. Billard, A. Ouadi, E. Jobin, J. Champion, C. Gaillard, S. Georg, Understanding the extraction mechanism in ionic liquids: $UO_2^{2+}/HNO_3/TBP/C_4$mimTf_2N as a case study, Solvent Extr. Ion Exch. 29 (2011) 577–601.
[67] M. Bonnaffé-Moity, A. Ouadi, V. Mazan, S. Miroshnichenko, D. Ternova, S. Georg, M. Sypula, C. Gaillard, I. Billard, Comparison of uranyl extraction mechanisms in an ionic liquid by use of malonamide or malonamide-functionalized ionic liquid, Dalton Trans. 41 (2012) 7526–7536.
[68] C. Gaillard, M. Boltoeva, I. Billard, S. Georg, V. Mazan, A. Ouadi, Ionic liquid-based uranium (VI) extraction with malonamide extractant: cation exchange vs. neutral extraction, RSC Adv. 6 (2016) 70141–70151.
[69] J. Mathur, P. Ruikar, M.B. Krishna, M. Murali, M. Nagar, R. Iyer, Extraction of Np (IV), Np (VI), Pu (IV) and U (VI) with amides, BEHSO and CMPO from nitric acid medium, Radiochim. Acta 73 (1996) 199–206.
[70] J. Rey, S. Dourdain, L. Berthon, J. Jestin, S. Pellet-Rostaing, T. Zemb, Synergy in Extraction System Chemistry: Combining Configurational Entropy, Film Bending, and Perturbation of Complexation, Langmuir 31 (2015) 7006–7015.
[71] M. Špadina, J.F. Dufrêche, S. Pellet-Rostaing, S. Marčelja, T. Zemb, Molecular Forces in Liquid-Liquid Extraction, Langmuir 37 (2021) 10637–10656.
[72] H. Friedman, L. Toth, Absorption spectra of Np (III),(IV),(V) and (VI) in nitric acid solution, J. Inorg. Nucl. Chem. 42 (1980) 1347–1349.
[73] J.P. Hessler, W. Carnall, Optical properties of actinide and lanthanide ions, in, ACS Publications, 1980.
[74] W. Carnall, G. Liu, C. Williams, M. Reid, Analysis of the crystal-field spectra of the actinide tetrafluorides. I. UF_4, NpF_4, and PuF_4, J. Chem. Phys. 95 (1991) 7194–7203.

[75] S. Edwards, F. Andrieux, C. Boxall, M. Sarsfield, R. Taylor, D. Woodhead, Neptunium (IV)-hydroxamate complexes: their speciation, and kinetics and mechanism of hydrolysis, Dalton Trans. 48 (2019) 673–687.
[76] D.C. Sonnenberger, J.G. Gaudiello, Cyclic voltammetric study of organoactinide compounds of uranium (IV) and neptunium (IV). Ligand effects on the M (IV)/M (III) couple, Inorg. Chem. 27 (1988) 2747–2748.
[77] A. Sengupta, M.S. Murali, P.K. Mohapatra, M. Iqbal, J. Huskens, W. Verboom, Extracted species of Np (IV) complex with diglycolamide functionalized task specific ionic liquid: diffusion, kinetics and thermodynamics by cyclic voltammetry, J. Radioanal. Nucl. Chem. 304 (2015) 563–570.
[78] M. Špadina, K. Bohinc, T. Zemb, J.F. Dufrêche, Synergistic solvent extraction is driven by entropy, ACS Nano 13 (2019) 13745–13758.